VIS: the visible imager for Euclid

Mark Cropper, A. Refregier, P. Guttridge, O. Boulade, J. Amiaux, et al.

Mark Cropper, A. Refregier, P. Guttridge, O. Boulade, J. Amiaux, D. Walton, P. Thomas, K. Rees, P. Pool, J. Endicott, A. Holland, J. Gow, N. Murray, A. Amara, D. Lumb, L. Duvet, R. Cole, J.-L. Augueres, G. Hopkinson, "VIS: the visible imager for Euclid," Proc. SPIE 7731, Space Telescopes and Instrumentation 2010: Optical, Infrared, and Millimeter Wave, 77311J (5 August 2010); doi: 10.1117/12.857224

Event: SPIE Astronomical Telescopes + Instrumentation, 2010, San Diego, California, United States

VIS: the visible imager for *Euclid*

Mark Cropper*[*a], A. Refregier[b], P. Guttridge[a], O. Boulade[b], J. Amiaux[b], D. Walton[a], P. Thomas[a], K. Rees[a], P. Pool[c], J. Endicott[c], A. Holland[d], J. Gow[d], N. Murray[d], A. Amara[e], D. Lumb[f], L. Duvet[f], R. Cole[a], J-L Augueres[b], G. Hopkinson[g]

[a]Mullard Space Science Laboratory, University College London, Holmbury St Mary, Dorking Surrey RH5 6NT, United Kingdom;

[b]Service d'Astrophysique, Commissariat à l'Énergie Atomique, Orme des Merisiers, Bat 709, 91191 Gif sur Yvette, France;

[c]e2v technologies plc, 106 Waterhouse Lane, Chelmsford, Essex CM1 2QU, United Kingdom;

[d]Centre for Electronic Imaging, Planetary and Space Sciences Research Institute, The Open University, Walton Hall, Milton Keynes, MK7 6AA, United Kingdom;

[e]ETH Hoenggerberg Campus, Physics Department, HIT J 12.2, CH-8093 Zurich, Switzerland;

[f]Research and Scientific Support Department, European Space Research and Technology Centre, Keplerlaan 1, PO Box 299, 2200 AG Noordwijk, The Netherlands;

[g]Surrey Satellite Technology Ltd., Rayleigh House, 1 Bat & Ball Road, Sevenoaks, Kent, TN14 5LJ, United Kingdom.

ABSTRACT

Euclid-VIS is a large format visible imager under investigation for the ESA *Euclid* space mission in their Cosmic Vision program. Together with the near infrared photometer (NIP) it forms the basis of the weak lensing measurements of *Euclid*. VIS will image in a single $r+i+z$ band from 550-920 nm over a field of view of ~0.5 deg^2. Over 4 exposures totalling 1800 sec, VIS will reach to V=24.9 (10σ) for sources with extent ~0.3 arcsec. The image sampling is 0.1 arcsec. VIS will provide deep imaging with a tightly controlled and stable PSF over a wide surcey area of of 20000 deg² to measure the cosmic shear from over 2 billion galaxies to high levels of accuracy, from which the cosmological parameters will be measured. In addition, VIS will also provide a legacy deep imaging dataset of unprecedented spatial resolution over the entire extra-Galactic sky. Here we will present the results of the study carried out by the *Euclid* Imaging Consortium during the *Euclid* Assessment Phase.

Keywords: Astronomy, satellites, charge-coupled device imagers, *Euclid*, dark energy.

1. INTRODUCTION

We stand at the threshold of a new conceptual understanding of the physical universe, as the subject did a century ago when classical physics was transformed by general relativity and quantum mechanics. In the current "concordance model" of the Universe, three quarters of its mass consists of Dark Energy, and one fifth of Dark Matter. *Euclid* is one of three candidate missions in ESA's Cosmic Vision programme (of which two will be selected for launch in 2017/2018) designed to make the most exquisitely accurate measurements of Dark Energy, to explore what it is, and to quantify precisely its role in the evolution of the Universe. *Euclid* will additionally measure and elucidate the nature of Dark Matter. If, instead, the concordance model is incorrect and our fundamental ideas about gravity need revision, *Euclid* will also test the validity of many of these modified gravity theories. Until there is high precision data to put these new theoretical frameworks to the test, real progress will be limited. *Euclid* will be one of the most powerful tools in this quest, one in which the systematics will be controlled to an unprecedented accuracy through the combination of different cosmological approaches and technical capability.

* msc@mssl.ucl.ac.uk; www.mssl.ucl.ac.uk

Space Telescopes and Instrumentation 2010: Optical, Infrared, and Millimeter Wave, edited by Jacobus M. Oschmann Jr., Mark C. Clampin, Howard A. MacEwen, Proc. of SPIE Vol. 7731, 77311J · © 2010 SPIE · CCC code: 0277-786X/10/$18 · doi: 10.1117/12.857224

Besides these studies in physics and cosmology, *Euclid* will provide a truly colossal legacy dataset over the whole sky, with optical imaging at 0.25 arc second spatial resolution to very faint limits (R~25 at 10σ), infrared imaging in 3 bands to similar limits and only slightly worse spatial resolution, and spectra and redshifts of 150 million galaxies to H~20 (fainter for emission line objects). A dataset of this size will be used by scientists worldwide in a wide range of contexts, and it will have huge scientific and public impact.

This paper discusses the Visible Imager (VIS) on *Euclid*, as envisaged at the end of the Assessment Phase (end-2009), updating the position at the beginning of that phase[1]. VIS is complemented by the Near Infrared Spectrometer (NIS) and Near Infrared Photometer (NIP) described in companion papers[2,3]. The overall scientific aims of *Euclid*, an overview of the mission and the translation to instrumental requirements are also available in this procedings[4,5].

2. PERFORMANCE REQUIREMENTS

2.1 Science aims

The main task of VIS is to carry out Weak Lensing measurements[4,5]. The Dark Matter (and ordinary matter) aggregates under the influence of gravity as the universe expands. These overdensities bend light from background objects, so that they appear distorted (weak gravitational lensing). The mass distribution can be reconstructed from the statistical averages of the shapes of background galaxies distorted by this effect, so this is how *Euclid* maps Dark Matter. Further, by using galaxies further and further away, the characteristics can be determined of the rate at which the agglomeration has occurred. This is directly affected by the expansion history of the Universe, which appears at more recent times to be increasingly driven by Dark Energy, so the characteristics of the Dark Energy can consequently also be constrained.

While there is a chain of inferences, in particular the successive removal of the foreground distortions to measure the more distant (and hence from earlier times) distortions, Weak Lensing is considered to be probably the most powerful technique to determine the characteristics of Dark Matter and Dark Energy[6,7]. To accomplish this task requires very large surveys, to ensure a sufficient number of sources and to overcome the natural variations within the Universe, and, also, extremely precise measurements of galaxy shapes. Systematic effects must be deeply understood and a prerequisite for this is calibrations of the highest quality.

Table 1: VIS requirements

Visible Shape Measurement Channel		
Spectral band	1 broad red band	R+I+Z (550– 920nm)
PSF	Size (FWHM 800nm)	Azimuthal average between 0.18 and 0.23 arcsec
	Sampling (at 800 nm)	CCD pixelsize = 0.1 arcsec
	Complexity	'Well behaved' (see text)
	Ellipticity	Less than 5% target on the full FoV < 20% as a maximum
	Stability	Ellipticity and FWHM rms variation less than 0.02% over 50 arcmin^2 (corresponding to 50 calibration stars)
	Chromatic	Wavelength dependence of PSF 'calibratable'
Image Quality	Cosmetics	< few % of bad pixels per exposure
	Linearity	Instrument calibratable for S/N 1-1000
	Distortion on 1" scale	< 1% anywhere in the FoV calibrated at 0.1% level
	Diffuse straylight	Stray light level less than 20% of zodiacal background at the ecliptic poles
Survey Geometry	Survey Area	20 000 deg^2 extragalactic, contiguous
	Galaxy distribution	40 galaxies/amin^2 usable for WL with a median redshift z_m>0.8
Systematics	Shear measurement	shear systematics variance $\sigma_{sys}^2 < 10^{-7}$

2.2 VIS characteristics

VIS therefore requires a large field of view sampled sufficiently finely to measure typical galaxy shapes. To cover most of the extra-Galactic sky in a reasonable mission duration (4-5 years) the field of view must be ~0.5 deg^2. To sample galaxies with typical sizes 0.3–0.4 arcsec, pixel sizes of 0.1 arcsec and smaller are required. To minimise the mass of the focal plane, pixels must be as small, consistent with sufficient full well capacity so that there is sufficient dynamic range (otherwise even faint images will saturate) and within a proven technological capability. These requirements are met with a focal plane of 36 CCDs, each of 4kx4k pixels, each 12µm square. We have considered other technologies, in particular infrared arrays such as those in the NIP and NIS operated in the visible band, and Active Pixel Sensors, but none of these have the requisite performance characteristics or track record in space for such a large focal plane.

Combined with the NIP infrared measurements (which are however more coarsely sampled) and data from the ground, the Weak Lensing measurements do not require VIS to provide multicolour information within the optical band, at least to the current level of understanding[8]. Measurements of distant galaxies at blue wavelength suffer more from the inhomogeneity of galaxies in the ultraviolet (shifted by the expansion of the Universe into the visible band). VIS therefore implements a single broad red band. Beyond these broad top-level requirements, VIS requires a shutter and calibration unit for flat-fielding the detector.

The more detailed requirements as captured in the Science Requirements Document[9] for VIS are tabulated in Table 1.

3. INTERFACES

3.1 Optical interface

Euclid has a 1.2m 3-mirror telescope, with the third mirror providing corrections to the intermediate Cassegrain focus. The VIS and NIP field selected from half of the field of view, the other half allocated to NIS. The VIS and NIP beams are split by a dichroic, working in reflection for VIS to produce a bandpass of 550 to 920nm with ~5nm band edges. To avoid low-level ghost images from internal reflections, especially as the rays incident on the focal plane are not telecentric, there are no other filters or optics in VIS, except for folding mirrors. The entrance pupil is 1.19m, central obscuration is 0.406m and the final focal ratio is f/20.8. This provides a plate scale of 0.1 arcsec per 12µm pixel, and a field of view of 1.058°x0.534°, or just over 0.5 square degrees. The optical performance is diffraction limited over the entire field, as shown in Figure 1.

Field	RMS spot radius (µm)	WFE in nm
1	3.7	18.3
2	3.2	14.28
3	3.7	18.3
4	2.5	13.14
5	3.5	18.24
6	2.5	13.14
7	3.6	17.94
8	1.6	7.02
9	**3.6**	17.94

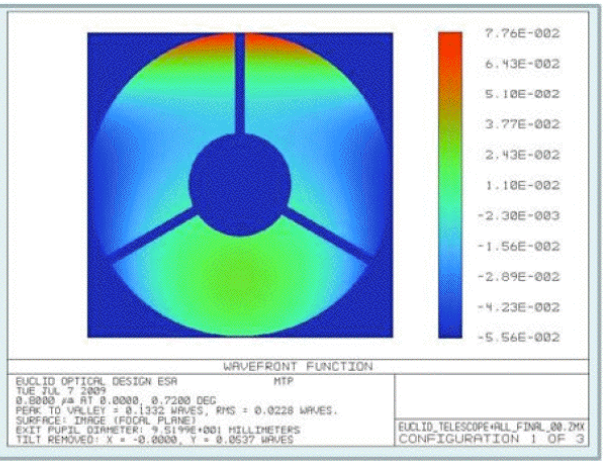

Figure 1: Wavefront error over the VIS field of view. For a reference wavelength of 600nm the as-designed wavefront error is less than λ/30.

3.2 Thermal and mechanical

VIS is supported by the payload module structure in the space below the telescope, with separate interfaces for the focal plane and the shutter/calibration unit. The *Euclid* payload module is cold, ~150K, to facilitate the near infrared instrument performance. This is also suitable for the operation of the VIS CCDs, which show optimum charge transfer

efficiency at this temperature (see section 5.3). On the other hand, for reasons of device operating conditions, the CCD detection chain electronics must be maintained at a temperature of 250K.

3.3 Electrical interfaces

As with the other *Euclid* instruments, VIS is connected to cold-redundant Payload Data Handling Units (PDHU)[10] through Spacewire interfaces, providing data and command links. There are also LVDS interfaces for sychronisation and timing. The PDHU is responsible for data compression and communication to the on-board command and control systems and mass memory unit. The PDHU interfaces to a Payload Mechanisms Control Unit (PCMU) which actuates the VIS shutter and calibration unit.

Partially-conditioned 28V power is provided by a Power Control and Distribution Unit (PCDU), also in cold-redundancy.

4. DESIGN

4.1 overview

Photons within the broad red bandpass (effectively SDSS $r+i+z$[11]) are detected through an array of 9x4 CCDs, each of which is a CCD203-82[12] manufactured by e2v Technologies, as shown in Figure 2. The CCDs are read out through 4 readout nodes at a rate of 200 kpix s^{-1}. The CCDs are held in a Detector Block matrix, as shown in Figure 2, which provides a 90% filling fraction of active Si.

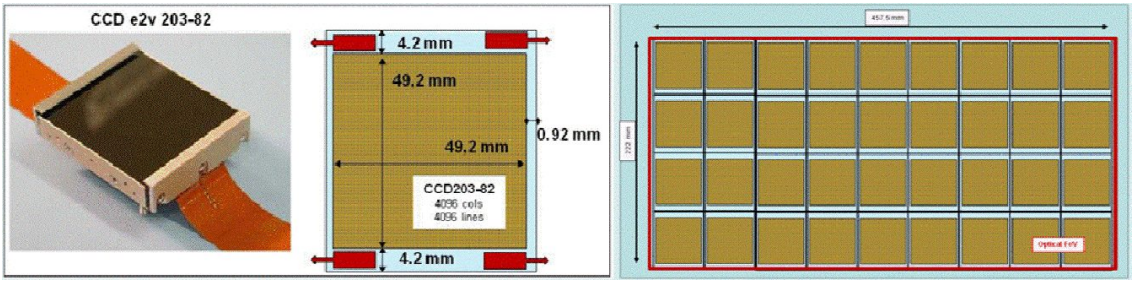

Figure 2: (left) The e2v CCD203-82 showing the active area. The package will be in SiC and the design optimised to improve buttability. (right) The layout of the active focal plane.

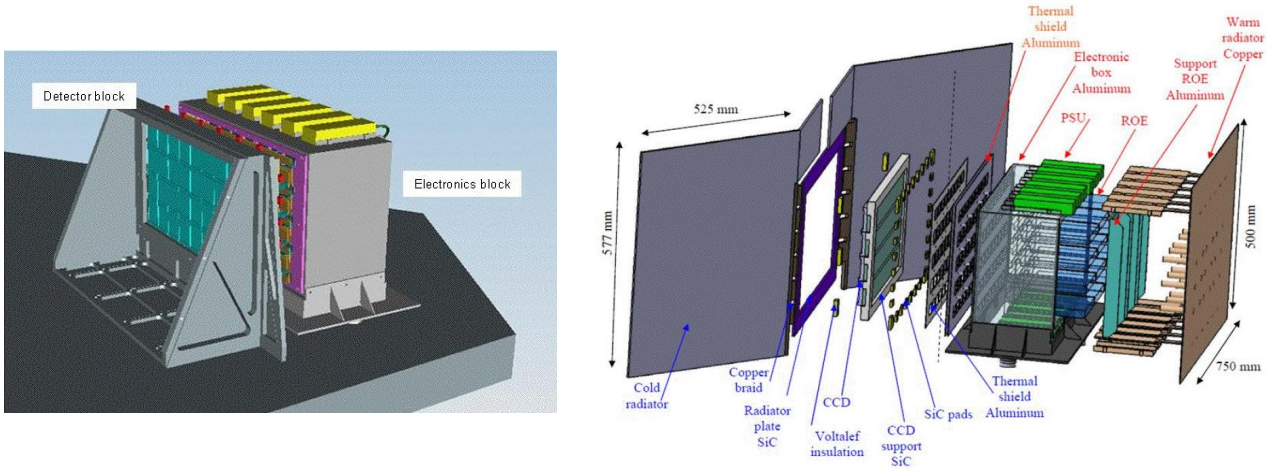

Figure 3: (left) The overall layout of the VIS Detector and Electronics Blocks, showing the CCD array held within the Detector Block. Power supply units are located above and below the ROEs within the Electronics Block. (right) Exploded view of the Detector and Electronics Blocks showing thermal hardware.

The detector array is maintained relative to the optical focal plane by a SiC structure. This is separated from the VIS Electronics Block, which is supported separately, with only the CCD electrical flexible interconnects between them (Figure 3). The electronics block holds twelve Readout Electronics (ROE – one for three CCDs), and their closely coupled power supply units (one per ROE). Within the support structure for the ROEs are thermal shields to isolate the cold CCDs from the warm ROEs. A radiator to space maintains the ROE thermal environment, while one coupled to the the detector block maintains the CCDs at a temperature of 150–160K.

The shutter and calibration source are separate units, one located near to the the dichroic and the other near the final fold mirror. The shutter allows the CCDs to remain in darkness while they are read out. The calibration source provides a quasi-uniform flat field illumination on the CCD to calibrate pixel-to-pixel variations.

4.2 Detection chain

The detection chain consists of the CCDs, ROEs and their associated power supply units. The architecture of the chain has been set up to ensure sufficient redundancy, while minimising the use of system resources. Manufacturability, testability and ease of access have also been important considerations. The tradeoff identified an optimal configuration of one ROE supporting three CCDs, each with four video chains (Figure 4), each with its own power supply unit. In order to minimise system noise levels, the power supply for each ROE is accommodated close to it on the outside of the Electronics Block. A single clocking and bias generation circuit is implemented for each CCD. Loss of one ROE results in loss of <10% of the focal plane, and the thermal perturbations are manageable. Within each ROE it is envisaged that individual CCDs may be lost without loss of the entire unit, providing further redundancy.

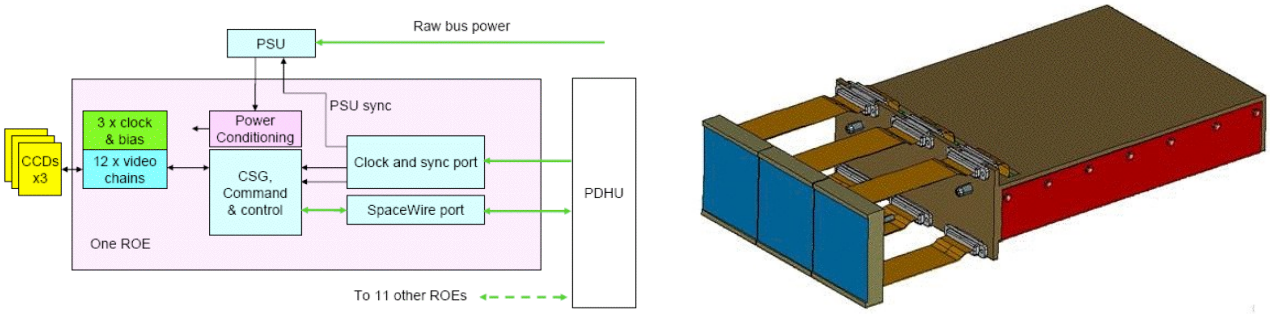

Figure 4: (left) The block diagram for an ROE, interfacing to 3 CCDs. (right) The mechanical packaging of an ROE with 3 CCDs.

Analog signals are converted to 16 bits resolution. In order to maintain thermal stability all circuitry remains powered during exposures. Care is taken in the design of mixed signal circuitry handling very low level analogue inputs, to prevent cross-talk and other noise pick-up: multi-layer printed circuit boards are used with separate ground planes for analogue and digital functions. System grounding and decoupling is carefully planned to prevent circulating currents in ground lines from introducing noise sources. All CCDs are read out synchronously, minimising radiated and conducted noise during the signal sampling with synchronisation effected through the LVDS interface. Data are transmitted through the Spacewire port to the PDHU, with Spacewire communication and command decoding, together with other digital functions such as clock sequence generation carried out in a single space-qualified FPGA per ROE.

Breadboard *Euclid* ROEs have already been designed and fabricated. These have representative board layouts and components, although in standard packaging suitable for use in vacuum equipment, and are currently in use for characterising CCD204-22 intra-pixel point spread functions and for quantifying the noise performance requirements of the ROE power supply units. The CCD204-22 is essentially a 4kx1k variant of the CCD203-82 with the same design and pixel structure, but with the addition of a charge injection register instead of the second readout register.

The packaging of the ROE and PSU electronics is designed to optimize conductive thermal paths while minimising the parasitic heat conduction to the CCDs. Special provision is made to allow the CCD interface connectors to float slightly, so they can be locked from the rear of the ROE after the integration of the CCDs.

4.3 VIS structure and thermo-mechanical aspects

The architecture of the assembly is modular, in two blocks (the Detector Block and the Electronics Block, Figure 3), to better deal with different constraints. The main design drivers that have been considered in the thermal design of the VIS structure are to ensure uniform 160K temperature on the CCDs with a maximum gradient across the focal plane of 3K, while at the same time providing for the removal of ~100W of power from the ROEs and their power supply units, keeping them around room temperature. At the same time it must provide thermal decoupling between these two blocks and to the remainder of the payload module. Figure 5 indicates that these thermal requirements are achievable. The mechanical drivers are to hold the CCDs at the VIS focus and the ROEs with sufficient stiffness within a tight mass budget, while allowing for coefficient of thermal expansion mismatch. Ease of assembly, adjustment and maintenance is also a high priority.

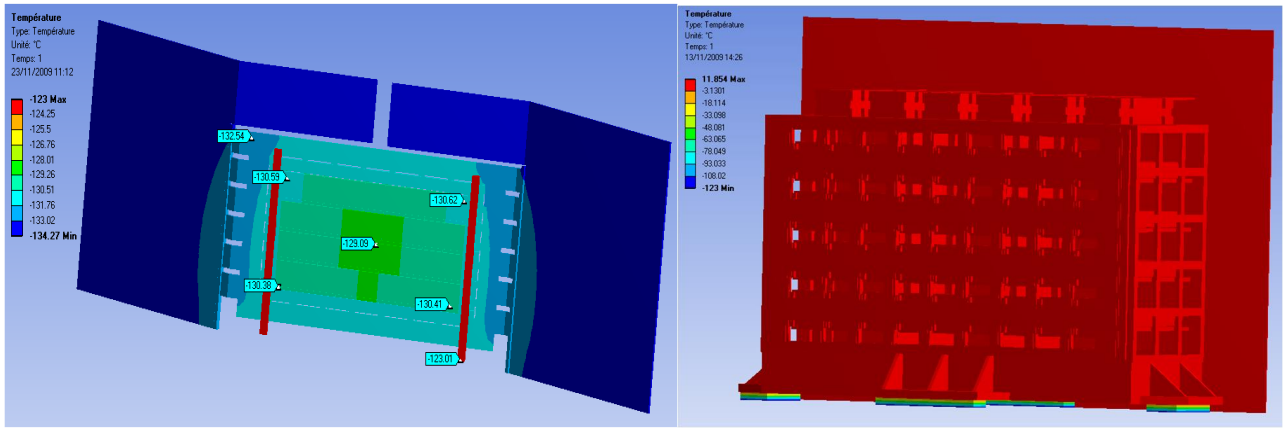

Figure 5: Thermo-mechanical analyses of the VIS Detector Block (left), showing uniformity within the focal plane to within 1°C, and (right) of the Electronics Block showing that the ROEs operate at temperatures above 0°C.

The CCD packaging is SiC, and most components of the Detector Block are also SiC to ensure matching of thermal characteristics. Most of the structural material in the Electronics Block is Aluminium. The radiator sizes are 0.7 m^2 for the Detector Block, and 0.375 m^2 for the electronics block. Under 26 g static loads, maximum displacements within the Detector Block are 0.4 mm and stresses below 57 MPa at the Detector Block to the payload module interface. For the Electronics Block, maximum displacement is 0.4 mm and maximum local stresses of 450 MPa are reached. First eigenfrequencies are at 280 Hz for the Detector Block and 80 Hz for the Electronics Block. This last eigenfrequency is too low, and requires further work to increase stiffness.

5. PARTICULAR ISSUES

5.1 Operational scheme

VIS will take multiple exposures of each part of the sky. While this increases the data rate, it is necessary in order to sample each galaxy and star profile multiple ways, to ensure sky coverage covering over gaps between detectors, to mitigate against radiation effects (Section 5.3 below) and to permit the identification and subtraction of cosmic ray events. These multiple exposures must be coordinated with the NIP and NIS observations and are described in more detail elsewhere[4].

5.2 The VIS point spread function

In order to measure the shape of weakly lensed galaxies to the level of accuracy required[5], the end-to-end point spread function (PSF) of the VIS system must be finely characterised. The PSF is composed of the optical PSF, the spacecraft pointing jitter and the detector internal charge spread convolved together, and sampled on the CCD pixel grid.

The internal charge spread within the CCDs will depend on their particular operation, and in particular the number of phases held high during the integration. These define the shape of the electrical potential in the column direction, while in the row direction the potential is defined by the column stops. The shape of the PSF is therefore slightly non-

axisymmetric, which adds ellipticity aligned with the pixel grid to the measured galaxy shapes. These effects are being quantified using CCD204-22 and the flight-like prototype ROEs developed during the Assessment Phase.

5.3 Radiation

Radiation damage effects in electronics and detectors at the orbit of *Euclid* near the L2 point are largely the result of Solar ions with ~MeV energies. These cause lattice damage in the Si within the pixels and readout registers, creating traps for electrons (or holes) when the CCD is read out. This leaves a charge trail behind each image as it is moved down the CCD column, and then another in the orthogonal direction as it is transferred along the readout register (Figure 6). The radiation damage effect is parameterised initially through a quantity called the Charge Transfer Inefficiency (CTI), which measures the fraction of charge lost after the pixel charge contents have been clocked to the readout register.

These effects are particularly relevant to *Euclid* VIS, because they change the shape of the image, directly affecting the primary quantity to be measured. A substantial programme is in place to understand and quantify them, and to introduce ameliorating measures into the CCD development programme (Section 8), where these might be possible. This includes radiation testing and characterisation, development of software models of varying complexity and of software algorithms for the final data analysis[13]. Many parameters need to be determined for inclusion in the models, in particular the time constants and cross sections of the different trap species, and the beneficial impacts of a non-zero optical background (mostly arising from Zodiacal light) and charge injection have to be quantified. The multi-exposure strategy (dithering) in Section 5.1 above is an important ingredient in isolating the effect, as each source will be exposed at different locations on the CCD with consequent trails of different extents.

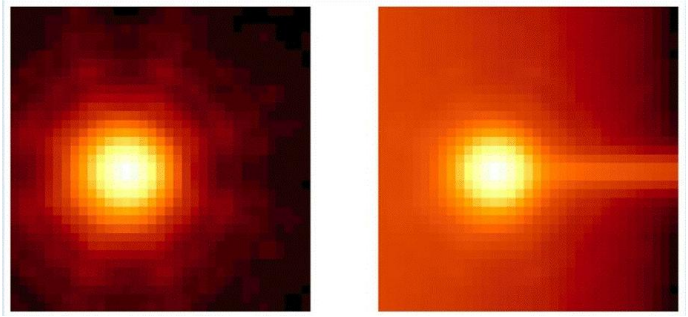

Figure 6: The effect of radiation damage in the CCD. The figure on the left is a simulated galaxy through the *Euclid* system without radiation damage (O. Boulade, CEA Saclay using code from A. Short, ESA) and the right shows the image with radiation damage and cosmic background included when the CCD is read out to the left side of the image. Both are on a log intensity scale to show low level effects.

It is clear that radiation damage will be a critical issue for VIS, and full end-to-end performance predictions will require continuously increasing fidelity to quantify its impact.

6. PERFORMANCE

Radiometric modelling predicts that VIS will reach AB magnitude 24.9 (10σ) in the $r+i+z$ band from three exposures of 450 sec. Most sources will be covered by 4 exposures from the dither pattern. Detector noise (mostly readout noise) will be $<6e^-$. Stellar sources saturate at R=16.9.

End-to-end simulations predict that the system PSF will have a full-width-half-maximum 0.16 arcsec, with a 0.22 arcsec 50% encircled energy width. The intrinsic ellipticity (using a quadrupole definition) is 0.025.

7. BUDGETS

The top-level budgets are presented in Table 2.

Table 2: Top level budgets

mass, excluding shutter and calibration unit	62 kg (including 20% margins)
radiator masses	51.6 kg (including 20% margins)
shutter and calibration unit masses	12.4 kg (including 20% margins)
power, excluding shutter and calibration unit	112W continuous primary power (measured)
shutter actuation power	14.4W
calibration unit power	1W
telemetry	497 Gbit/day (factor 2.8 compression)

8. FUTURE DIRECTIONS

Euclid is undergoing continuous development as it moves into the Definition Phase. The e2v CCD203-82 is being enhanced in a modest programme to incorporate charge injection structures, and to improve the serial register charge transfer efficiency. Tradeoffs are being considered whether a reduction in the detector array from 36 to 30 CCDs can be countenanced without too-significant performance degradation and survey duration extension. In addition, consideration is being given to the feasibility of incorporating two filters in VIS rather than the single broad band.

REFERENCES

[1] Booth, J., Cropper, M., Eisenhauer, F., Refregier, A. and the *DUNE* Collaboration, "The focal plane instrumentation for the DUNE mission", Proc. SPIE, Vol. 7010, 70101D (2008)

[2] Schweitzer, M. et al "NIP: the near-infrared imaging photometer for Euclid", these proceedings, (2010)

[3] Valenziano, L. et al "The E-NIS instrument on-board the ESA Euclid Dark Energy Mission: a general view", these proceedings, SPIE, (2010)

[4] Laureijs, R. et al "The Euclid Mission", these procedings SPIE (2010)

[5] Amiaux, J. et al "Euclid imaging channels: from science to system requirements", these proceedings, SPIE, (2010)

[6] Report of the ESA-ESO Working Group on Fundamental Cosmology, September 2006 http://www.stecf.org/coordination/esa_eso/cosmology/report_cover.pdf

[7] Report Of The Dark Energy Task Force, 6 June 2006 http://www.nsf.gov/mps/ast/aaac/dark_energy_task_force/report/detf_final_report.pdf

[8] Cypriano, E., Amara, A., Voigt, L., Bridle, S., Abdalla, F., Réfrégier, A., Seiffert, M., Rhodes, J. "Cosmic shear requirements on the wavelength dependence of telescope point spread functions", MNRAS, in press, 2010

[9] *Euclid* Science Study Team, "Euclid Science Requirements Document", issue 3 revision 2, DEM-SA-Dc-00001, 24 August 2009

[10] di Giorgio, A., et al "The data handling unit of the Euclid imaging channels: from the observational requirements to the unit architecture", these proceedings, SPIE, (2010)

[11] SDSS Data Release 7: Imaging camera parameters and description http://www.sdss.org/dr7/instruments/imager/index.html - filters

[12] e2v CCD203-82 data sheet http://www.e2v.com/assets/media/files/documents/imaging-space-and-scientific-sensors/33-CCD203_data_sheet_2a.pdf

[13] Massey, R., Stoughton, C., Leauthaud, A., Rhodes, J., Koekemoer, A., Ellis, R., Shaghoulian, E., "Pixel-based correction for Charge Transfer Inefficiency in the Hubble Space Telescope Advanced Camera for Surveys", MNRAS 401, 371 (2010)